Inorg. Chem. **2006**, *45*, 66–73

Mercury(II) Cysteine Complexes in Alkaline Aqueous Solution

Farideh Jalilehvand,*,† Bonnie O. Leung,† Maryam Izadifard,† and Emiliana Damian‡

Department of Chemistry, University of Calgary, Calgary, Alberta, T2N 1N4 Canada, and Arrhenius Laboratory, Deparment of Structural Chemistry, Stockholm University, Stockholm, SE-106 91 Sweden

Received June 2, 2005

Mercury(II) complexes with L-cysteine (H_2Cys) in alkaline aqueous solutions have been structurally characterized by means of extended X-ray absorption fine structure (EXAFS) spectroscopy. The distribution of $[Hg(Cys)_n]$ (n = 2, 3, and 4) species in ~0.09 mol dm^{-3} mercury(II) solutions with H_2Cys/Hg^{II} ratios varying from 2.2 to 10.1 has been evaluated by fitting linear combinations of simulated EXAFS functions for the separate complexes to the experimental EXAFS data, aided by ^{199}Hg NMR and Raman results. For the $[Hg(Cys)_2]^{2-}$ and $[Hg(Cys)_3]^{4-}$ complexes and the novel four-coordinated $Hg(Cys)_4$ species that dominates in solutions with excess of cysteine (H_2Cys/Hg^{II} > 5), the mean Hg–S bond distances were found to be 2.35(2), 2.44(2), and 2.52(2) Å, respectively. The minor amount of the linear $[Hg(Cys)_2]^{2-}$ complex that can still be discerned in solutions with ratios up to H_2Cys/Hg^{II} = 5 was derived from the distinct S–Hg–S symmetric stretching Raman band at 334 cm^{-1}. From ^{199}Hg NMR spectra, the chemical shift of the $Hg(Cys)_4$ species was estimated to –340 ppm with an amount exceeding 85% in the highest excess of cysteine, consistent with the EXAFS data.

Introduction

Inorganic mercury exposure is known to cause toxic effects because the affinity of mercury(II) ions to thiol (sulfhydryl) groups in proteins leads to unspecific inhibition of cellular enzymes, affecting membrane permeability and nerve conduction.[1] Several types of cysteine derivatives (e.g., penicillamine (3,3′-dimethylcysteine) and *N*-acetyl cysteine) form soluble complexes and have been suggested as possible detoxification agents.[2] For understanding the transportation processes of mercury(II) in physiological systems, structural studies of the strong interaction with the thiol groups of cysteine can serve as models for cysteine-containing proteins and peptides.[3,4] In fact, the toxicity was found to increase with more severe renal injury when L-cysteine was administered together with inorganic Hg^{II} than with Hg^{II} exposure alone.[3b]

Mercury(II) often forms very stable linear complexes with two sulfur donor ligands. However, the Hg^{II}−thiol bonds are labile, and for higher Hg−S coordination numbers, the structures are flexible, often with distorted trigonal or tetrahedral coordination figures.[5] During the past decade, new insight into the Hg^{II}−thiol coordination environment has been obtained by structural analyses on metalloregulatory proteins (MerR) and cysteine-rich metallothioneins (MT). Low intensity UV absorption bands, attributed to ligand to metal (S → Hg) charge transfer of trigonal or distorted tetrahedral Hg^{II}−MerR/MT complexes at physiological pH appear as characteristic shoulders in the region of 280−310 nm.[6−8] In the Hg−MerR protein, EXAFS spectroscopy revealed $Hg^{II}-S_3$ coordination to cysteine residues in a receptor site with the mean Hg−S bond distance 2.43(2) Å.[8−10] For the metallothionein Hg_7MT, two separate EXAFS studies yielded somewhat different results: (1) $Hg^{II}-S_3$ coordination with the mean bond distance 2.42(2) Å[11] and (2) a $Hg^{II}-S_4$ structure with two short Hg−S bonds, 2.33(2) Å, and two long Hg−S interactions at ~3.4 Å, in Hg_7MT formed by

* To whom correspondence should be addressed. E-mail: faridehj@ucalgary.ca.
† University of Calgary.
‡ Stockholm University.

(1) Hughes, W. L. *Ann. N Y. Acad. Sci.* **1957**, *65*, 454.
(2) Martindale, W. *The Extra Pharmacopoeia*, 31st ed.; Royal Pharmaceutical Society: London, 1996; pp 989−992.
(3) (a) Bridges, C. C.; Bauch, C.; Verrey, F.; Zalups, R. K. *J. Am. Soc. Nephrol.* **2004**, *15*, 663. (b) Zalups, R. K.; Barfuss, D. W. *Toxicology* **1996**, *109*, 15.
(4) Park, J. D.; Liu, Y.; Klaassen, C. D. *Toxicology* **2001**, *163*, 93.
(5) Cheesman, B. V.; Arnold, A. P.; Rabenstein, D. L. *J. Am. Chem. Soc.* **1988**, *110*, 6359.
(6) Vašák, M.; Kägi, J. H. R.; Hill, H. A. O. *Biochemistry* **1981**, *20*, 2852.
(7) Beltramini, M.; Lerch, K.; Vašák, M. *Biochemistry* **1984**, *23*, 3422.
(8) Watton, S. P.; Wright, J. G.; MacDonnell, F. M.; Bryson, J. W.; Sabat, M.; O'Halloran, T. V. *J. Am. Chem. Soc.* **1990**, *112*, 2824.
(9) Wright, J. G.; Tsang, H. T.; Penner-Hahn, J. E.; O'Halloran, T. V. *J. Am. Chem. Soc.* **1990**, *112*, 2434.
(10) Penner-Hahn, J. E.; Tsang, H. T.; O'Halloran, T. V.; Wright, J. G. *Physica B* **1989**, *158*, 117.
(11) Hasnain, S. S. *Top. Curr. Chem.* **1988**, *147*, 73.

10.1021/ic0508932 CCC: $33.50
Published on Web 12/13/2005

the addition of Hg^{II} to Zn_7MT at pH = 7.[12] In a similar study on $Hg_{18}MT$, formed by adding $Hg(NO_3)_2$ to Zn_7MT at pH = 2, a distorted trigonal Hg^{II} coordination was proposed, with two Hg−S bonds at 2.42(2) Å and one Hg−Cl bond at 2.57(3) Å.[12]

A survey of mercury(II) thiolate crystal structures established distinct ranges for the Hg−S bond distances: 2.32−2.36 Å for linear $[M(SR)_2]$ complexes, 2.42−2.44 Å for trigonal $[M(SR)_3]^-$ species, and 2.52−2.54 Å for tetrahedral $[M(SR)_4]^{2-}$ species. The strong correlation between the coordination number and the mean Hg−S bond distance, with an increase of ∼0.1 Å for each added ligand, is useful for structural interpretation of the EXAFS results.[13−16]

In aqueous solution, both the −SH and the $-NH_3^+$ groups of the cysteine ($H_2Cys = HSCH_2CH(NH_3^+)COO^-$) species simultaneously start to deprotonate at about pH 8.5, and at pH values above ∼10.5, the Cys^{2-} species becomes dominating.[17] Conflicting stability constants have been reported for the aqueous Hg^{II}−cysteine system for the formation of, for example, the Hg(Cys), $Hg(Cys)_2$, Hg(HCys)(Cys), and $Hg(HCys)_2$ species, although in all studies the $[Hg(Cys)_2]^{2-}$ complexes are found to have high stability in alkaline solutions.[5,18−21]

Various suggestions have been made for the Hg^{II}−cysteine bond modes, in addition to the well-known strong preference for the thiol group. From a potentiometric study, cysteine was proposed to act as a tridentate ligand in a solution with a ratio of $H_2Cys/Hg^{II} = 2$.[22] An IR spectrum of a concentrated alkaline solution, 0.5 mol dm^{-3} Hg^{II} in 2 mol dm^{-3} NaOD, ratio $H_2Cys/Hg^{II} = 2$, suggested coordination through the thiol and amino groups.[23] NMR studies (^1H and ^{13}C) resulted in Hg^{II}−thiol interactions for an acidic solution of bis(L-cysteinato)mercury(II) hydrochloride, $[Hg(HCys)(H_2Cys)]Cl\cdot 0.5H_2O$.[24] Another ^1H NMR study for acidic solutions with different H_2Cys/Hg^{II} ratios indicated Hg^{II}−S bonding with one or two cysteine ligands,[25] while ^{13}C NMR of alkaline 40−60 mmol dm^{-3} Hg^{II} solutions with ratios $H_2Cys/Hg^{II} > 2$ showed the formation of the $[Hg(Cys)_3]^{4-}$ complex.[5]

With the aim to structurally characterize the coordination and bonding of the dominating Hg^{II}−cysteine complexes existing in alkaline solutions, we performed a combined EXAFS, ^{199}Hg NMR, UV−vis, and Raman spectroscopic study. The stoichiometric H_2Cys/Hg^{II} ratio was systematically varied from 2.2 to 10.1, and the number of Hg^{II} species was evaluated using the Principal Component Analysis. The current paper presents the structures and ratios in aqueous solutions of the $[Hg(Cys)_2]^{2-}$, $[Hg(Cys)_3]^{4-}$, and also the novel four-coordinated $Hg(Cys)_4$ species. The charge of a $[Hg(Cys)_4]^{6-}$ complex may be reduced by protonation of the NH_2 group of the Cys^{2-} ligands at moderately alkaline pH values or by ion-pair formation, and therefore, the notation $Hg(Cys)_4$ is used.

These results are part of a systematic study of heavy metal ion complexes with cysteine, aiming to provide a basis for a better understanding of the properties of heavy metal ions in physiological systems and for detoxification treatments with the use of cysteine derivatives as complex-forming agents.

Table 1. Composition of the Hg^{II}−Cysteine Solutions[a]

solution	H_2Cys/Hg^{II} ratio	$[Hg^{2+}]_{tot}$[b]	$[ClO_4^-]$	$[H_2Cys]_{tot}$	pH
A	2.2	96	192	214	11.7
B	3.3	94	188	308	10.8
C	4.3	94	188	400	11.0
D	5.3	93	186	490	11.0
E	10.1	82	164	829	11.0
F	10.3	82	164	847	13.1
G	7.0	93	186	650	10.8
H	8.0	93	186	743	10.8
I	11.5	79	158	915	11.0
J	2.0	95	190	193	10.4

[a] Concentrations in mmol dm^{-3}. [b] $[Hg^{2+}]_{tot}$ from the ICP analysis is within ±4 mmol dm^{-3}.

Experimental Procedures

Sample Preparation. L-Cysteine, sodium hydroxide, and mercury(II) perchlorate hydrate, $Hg(ClO_4)_2\cdot xH_2O$ ($x = 3.26$), were used as obtained from Aldrich. All solutions were prepared under argon atmosphere using boiled oxygen-free water, monitoring the pH with a Corning Semi-Micro electrode calibrated with standard buffers. Cysteine (3−15 mmol) was dissolved in 12.5 mL of water at room temperature, giving pH ≈ 4.1. When 1.3 mmol of $Hg(ClO_4)_2\cdot xH_2O$ was added to the stirred solution, a white precipitate immediately formed, and the pH dropped to between 1 and 2, depending on the cysteine concentration. Dropwise addition of 6 mol dm^{-3} NaOH completely dissolved the precipitate at pH = 7.7. Six alkaline aqueous solutions with H_2Cys/Hg^{II} ratios of 2.2, 3.3, 4.3, 5.3, 10.1, and 10.3 (A−F in Table 1) were prepared in this way. The total Hg^{II} concentration was determined with accuracy within ±4 mmol dm^{-3}, by recording the emission at 194.2 nm using a Thermo Jarrell Ash AtomScan 16 inductively coupled plasma atomic emission spectrophotometer (ICP−AES). For measuring ^{199}Hg NMR spectra, new sets of the A−D solutions containing 10 vol % D_2O were prepared, as also the additional solutions G−I (Table 1).

The white precipitates from preparations with H_2Cys/Hg^{II} ratios 2.2 and 5.3 were filtered, washed with water and ether, and dried under vacuum. Elemental analyses for both solids were consistent with the ratio $H_2Cys/Hg^{II} = 2$, and DSC/ TGA analyses confirmed that the solids were water-free. Vibrational frequencies of perchlorate ions were absent in the IR and Raman spectra,[26] as also the

(12) (a) Jiang, D. T.; Heald, S. M.; Sham, T. K.; Stillman, M. J. *J. Am. Chem. Soc*. **1994**, *116*, 11004. (b) Lu, W.; Kasrai, M.; Bancroft, G. M.; Stillman, M. J.; Tan, K. H. *Inorg. Chem.* **1990**, *29*, 2561.
(13) Wright, J. G.; Natan, M. J.; MacDonnell, F. M.; Ralston, D. M.; O'Halloran, T. V. *Prog. Inorg. Chem.* **1990**, *38*, 323.
(14) Gruff, E. S.; Koch, S. A. *J. Am. Chem. Soc*. **1990**, *112*, 1245.
(15) Taylor, N. J.; Carty, A. J. *J. Am. Chem. Soc*. **1977**, *99*, 6143.
(16) Allen. Cambridge Structural Database (CSD), Version 1.7, 2004 release. Allen, F. H. *Acta Crystallogr*. **2002**, *B58*, 380.
(17) Wrathall, D. P.; Izatt, R. M.; Christensen, J. J. *J. Am. Chem. Soc.* **1964**, *86*, 4779.
(18) Berthon, G. *Pure Appl. Chem.* **1995**, *67*, 1117.
(19) Perkins, D. J. *Biochem. J.* **1953**, *55*, 649.
(20) McAuliffe, C. A.; Murray, S. G. *Inorg. Chim. Acta Rev.* **1972**, *6*, 103.
(21) Stricks, W.; Kolthoff, I. M. *J. Am. Chem. Soc.* **1953**, *75*, 5673.
(22) Lenz, G. R.; Martell, A. E. *Biochemistry* **1964**, *3*, 745.
(23) Shindo, H.; Brown, T. L. *J. Am. Chem. Soc.* **1965**, *87*, 1904.
(24) Neville, G. A.; Drakenberg, T. *Can. J. Chem.* **1974**, *52*, 616.
(25) Natusch, D. F. S.; Porter, L. J. *J. Chem. Soc. A* **1971**, 2527.
(26) (a) Nebgen, J. W.; McElroy, A. D.; Klodowski, H. F. *Inorg. Chem.* **1965**, *4*, 1796. (b) Hester, R. E.; Plane, R. A. *Inorg. Chem.* **1964**, *3*, 769.

−SH stretching band at about 2568 cm^{-1}, consistent with direct Hg−S coordination in a $[Hg(HCys)_2]$ coordination compound.[23] Anal. Calcd for $HgS_2C_6O_4N_2H_{12}$: C 16.27, H 3.19, N 6.33. Found (H_2Cys/Hg^{II} ratio 2.2): C 16.23, H 2.61, N 6.33. Found (H_2Cys/Hg^{II} ratio 5.3): C 16.63, H 2.83, N 6.54.

Raman and Electronic and ^{199}Hg NMR Spectroscopy. The solutions, contained in closed vials, were exposed for 90 min to the 1064 nm line (500 mW) from a YAG laser. The Raman spectra (about 2735 co-added scans) were recorded in the range of 100−3500 cm^{-1} with a 4 cm^{-1} resolution by means of a Bruker FRA 106 FT-Raman system equipped with a liquid-nitrogen cooled Ge-detector. Baseline correction was performed by subtracting the spectrum of vial plus pure water. For the Raman intensity calibration, the area of the perchlorate Cl−O symmetric stretching band at 933 cm^{-1} was correlated to the known perchlorate (ClO_4^-) concentration (Table 1). The peak area of the S−Hg−S symmetric stretching frequency of the $[Hg(Cys)_2]^{2-}$ complex at 334 cm^{-1} was then obtained in a curve fitting procedure (band shape 50:50 Gaussian/Lorentzian), by means of the GRAMS software package.

Electronic absorption spectra of solutions A−D were measured by means of a Varian Cary 219 double beam spectrophotometer at room temperature, with the solutions contained in quartz cells with a 1 mm path length. Three scans in the range of 200−400 nm were averaged, using the same concentration of cysteine in aqueous solution at pH = 11 as blank.

^{199}Hg NMR spectra of solutions A−D and G−I were collected on a Bruker Advance DRX-400 spectrophotometer equipped with a 5 mm broad band probe in the low frequency range (BBO probe). The external reference, saturated $HgCl_2$ in D_2O, was set to −1550 ppm.[13,27] The spectra were collected using a 30° pulse and zgdc30 pulse program with a sweep width of 1000 ppm and proton decoupling. All spectra were recorded at 300 K over 45 min with a 1 s delay (D1).

EXAFS Data Collection. Hg L_{III}-edge X-ray absorption spectra were recorded at the beamlines 4-1 and 2-3 of the Stanford Synchrotron Radiation Laboratory (SSRL), and at beamline 10-B at the Photon Factory (PF) of the High Energy Accelerator Research Organization, Tsukuba, Japan. Both facilities operated under dedicated conditions: SSRL at 3.0 GeV and 70−100 mA and PF at 2.5 GeV and 250−300 mA. At SSRL, harmonics from the Si[220] double crystal monochromator were rejected by detuning to 50% of maximum intensity at the end of the scan. At PF, the fully tuned Si[311] channel-cut monochromator prevents contamination with higher harmonics.

The measurements were performed in transmission mode, with nitrogen in the first ion chamber (I_0), and argon in the second (I_1) chamber, after the sample. The solid samples were finely ground, diluted with boron nitride, and enclosed between Mylar tapes; the solutions were held in 5 mm Teflon spacers between 4 μm X-ray polypropylene film windows. The energy scale was externally calibrated by assigning the first inflection point of the mercury L_{III}-edge absorption spectrum of crystalline $HgCl_2$ powder to 12284 eV, before averaging 3−4 scans for each sample.

EXAFS Data Analysis. The EXAFS oscillation was extracted using the WinXAS 3.1 program system.[28] The background absorption was subtracted using a first-order polynomial over the preedge region, followed by normalization of the edge step. The energy scale was converted to k-space, $k = [(8\pi^2 m_e/h^2)(E - E_0)]^{1/2}$, using a threshold energy of E_0 = 12285 eV. Above the edge, the atomic background contribution was removed by subtracting a seven-segment cubic spline.

Table 2. Parameters Used To Model EXAFS Spectra for $Hg(Cys)_n$ Species[a]

species	C.N.	R_{Hg-S} (Å)	$\sigma^2 \times 10^3$ (Å^2)
$[Hg(Cys)_2]^{2-}$	2*f*	2.32−2.36 [2.35]	3 [3]
$[Hg(Cys)_3]^{4-}$	3*f*	2.43−2.46 [2.44−2.45]	4−7 [6]
$Hg(Cys)_4$	4*f*	2.51−2.55 [2.52−2.53]	6−9 [8]

[a] ΔE_0 and S_0^2 values were fixed at 12 eV and 0.9, respectively. Best fits were obtained using values in brackets. (*f* = fixed value)

Table 3. Structural Parameters for the Hg^{II}−S Interactions in the Solid Compound and in the Alkaline Aqueous Solutions (See Figure 3), As Obtained from Least-Squares Fittings of the Fourier-Filtered Hg L_{III}-Edge $k^3 \cdot \chi(k)$ Data

	H_2Cys/Hg^{II} ratio	C.N.[a]	R (Å)[b]	σ^2 (Å^2)[c]	facility
solid[d]	2	2*f*	2.34	0.0028	SSRL 4-1
solution	2.2 (A)	2.05	2.36	0.0037	PF 10-B
	3.3 (B)	2.13	2.39	0.0069	SSRL 2-3
	4.3 (C)	2.73	2.44	0.0089	PF 10-B
	5.3 (D)	3.40	2.50	0.0087	SSRL 4-1
	10.1 (E)	3.48	2.50	0.0084	PF 10-B
	10.3 (F)	3.51	2.50	0.0090	SSRL 2-3

[a] Constant coordination number 2 for the solid, $S_0^2 = 0.9$ for the solutions; see Experimental Procedures). [b] Estimated error ±0.02 Å. [c] Estimated error ±0.0005 Å^2. [d] Precipitate formed when adding Hg^{II} to cysteine solutions (cf. Figure 1).

The EXAFS oscillation, $\chi(k)$, was modeled by means of the expression

$$\chi(k) = \sum_i \frac{N_i {S_0}^2}{k {R_i}^2} |f_{eff}(k)|_i \exp(-2k^2\sigma_i^2) \exp[-2R_i/\Lambda(k)] \sin[2kR_i + \phi_{ij}(k)] \quad (1)$$

The parameters are the following: the number N_i of backscattering atoms at the mean distance R_i from the absorber in the *i*th shell; the Debye−Waller parameter σ_i^2 related to the mean-square variation in a Gaussian distribution of distances around R_i; the scattering variable k; the effective amplitude function $|f_{eff}(k)|_i$; the total phase-shift $\phi_{ij}(k)$ of the absorber-scatterer pair; the photoelectron mean free path $\lambda(k)$; and the amplitude reduction factor S_0^2.

Ab initio calculated amplitude $f_{eff}(k)_i$, phase shift $\phi_{ij}(k)$, and mean free path $\lambda(k)$ functions were obtained by means of the FEFF 8.1 program,[29] for a mercury−cysteine complex derived from the $[Hg(CH_3)(HCys)]\cdot H_2O$ crystal structure.[30] Structural parameters for the Hg−S interaction were obtained by least-squares refinements of the theoretical model function $\chi(k)$, allowing R, σ^2, S_0^2, and ΔE_0 to float, to the k^3-weighted EXAFS oscillation over the k-range of 2.5−12 Å^{-1} (16 Å^{-1} for solids), after Fourier-filtering in the range of 1.30−3.20 Å. For the solid samples, a fixed coordination number yielded $S_0^2 \approx 0.9$ and ΔE_0 values between 12.2 and 12.5 eV. For the solutions, the S_0^2 value was held constant at 0.9 to allow refinements of the coordination number (Table 3). The ΔE_0 value was 12.2 eV for solution A and varied between 8.6 and 10.0 eV for solutions B−F. The accuracy of the mean bond distance R is estimated to be within ±0.02 Å, including systematic errors.

(27) Klose, G.; Volke, F.; Peinel, G.; Knobloch, G. *Magn. Res. Chem.* **1993**, *31*, 548.
(28) Ressler, T. *J. Synchrotron Rad.* **1998**, *5*, 118.
(29) (a) Zabinsky, S. I.; Rehr, J. J.; Ankudinov, A.; Albers, R. C.; Eller, M. J. *J. Phys. Rev. B* **1995**, *52*, 2995. (b) Ankudinov, A. L.; Rehr, J. J. *J. Phys. Rev. B* **1997**, *56*, R1712.
(30) Taylor, N. J.; Wong, Y. S.; Chieh, P. C.; Carty, A. J. *J. Chem. Soc., Dalton Trans.* **1974**, 438.

The Principal Component Analysis (PCA) procedure,[31] introduced in the EXAFSPAK program package,[32] was applied on the series of Fourier-filtered EXAFS oscillations obtained for the six solutions A−F (Table 1) over the k-range of 2.5−12 Å^{-1} and revealed the presence of three major components (cf. Figure S1 and Table S1).

To evaluate the relative amount of the major Hg^{II} species $Hg(Cys)_n$ (n = 2, 3, 4) in each solution, theoretical EXAFS functions were calculated by means of the WinXAS and FEFF 8.1 programs for the Hg−S interactions of $[Hg(Cys)_2]^{2-}$, $[Hg(Cys)_3]^{4-}$, and $Hg(Cys)_4$ standard species (Figure S2), using the parameters shown in Table 2 with $S_0^2 = 0.9$. Also, the ΔE_0 value was fixed at 12 eV, as for the solid $Hg(HCys)_2$ compound and for solution A. For the linear $[Hg(Cys)_2]^{2-}$ standard species, the Debye−Waller disorder parameter was fixed at 0.003 Å^2 for the Hg−S interaction, as for the solid $Hg(HCys)_2$ compound (cf. Table 3). The DATFIT program in the EXAFSPAK package was then used to fit the Fourier-filtered EXAFS oscillation of the solutions A−F to model functions consisting of linear combinations of the theoretical EXAFS functions of the standards. Distances below 2.34 Å for the linear S−Hg−S entity caused a distinct phase shift between the experimental EXAFS and the model function, especially for solution A. Similarly, for solutions D−F, distances above 2.54 Å for the four-coordinated species resulted in poor fits. The best fits were obtained for the mean Hg−S distances 2.35, 2.44−2.45, and 2.52−2.53 Å, with the Debye−Waller parameters 0.003, 0.006, and 0.008 Å^2 for the standards $[Hg(Cys)_2]^{2-}$, $[Hg(Cys)_3]^{4-}$, and $Hg(Cys)_4$, respectively. Systematic variation of the Hg−S distances within the ranges given in brackets in Table 2 induced variations in the values for the amount of each species by about ±10% (cf. Table 4).

Theoretical calculations were performed to ensure that the estimated Debye−Waller parameters for the standards were reasonable. Cartesian coordinates for these species were obtained from their optimized molecular geometries (Figure S2), using the VWN local density approximation (LDA) density functional in the Amsterdam Density Functional (ADF) program.[33] On the basis of the experimental Raman Hg−S symmetric stretching frequencies for $Hg(Cys)_2^{2-}$ (334 cm^{-1}), $[Hg(S\text{-}t\text{-}Bu)_3]^-$ (206 cm^{-1}), and $[Hg(SPh)_4]^{2-}$ (179 cm^{-1}),[13] their corresponding harmonic force constants were calculated to be 181.7, 69.1, and 52.2 N m^{-1}. These values resulted by means of the FEFF 8.1 program system in calculated Debye−Waller parameters for the $[Hg(Cys)_2]^{2-}$, $[Hg(Cys)_3]^{4-}$, and $Hg(Cys)_4$ species of 0.0027, 0.0064, and 0.0084 Å^2, respectively, which were in good agreement with our estimated values from EXAFS linear combination fitting.

Results and Discussion

EXAFS of Hg^{II}−Cysteine Solids. The EXAFS oscillations extracted for the solid precipitates from the acidic (pH < 2) solutions with H_2Cys/Hg^{II} ratios of 2.2 and 5.3 are quite similar. Their Fourier transforms display a single peak in the same position (Figure 1). The Hg−S bond distance of 2.34(2) Å obtained from least squares curve fittings to the EXAFS oscillations (Table 3) is in agreement with the mean value of 2.34 Å obtained for the nearly linear S−Hg−S entities of the $[Hg(HCys)(H_2Cys)]Cl\cdot 0.5H_2O$ crystal structure.[15] The Debye−Waller parameter (σ^2), describing the mean-square-variation in the mean Hg−S bond length due to the combined effect of thermal and positional disorder, is quite low. This suggests closely similar S−Hg−S bond lengths, as expected for a linearly two-coordinated $[Hg(HCys)_2]$ complex.

Table 4. EXAFS Analyses of the Relative Amount of $[Hg(Cys)_n]$ Species (n = 2, 3, 4) in Solutions A−F

model	species	% $[Hg(Cys)_2]^{2-}$	% $[Hg(Cys)_3]^{4-}$	% $Hg(Cys)_4$	av. R^a
I	Hg−S distance	2.35	2.44	2.52	
	A (2.2)	94	6		2.355
	B (3.3)	41	59		2.403
	C (4.3)	11	62	27	2.452
	D (5.3)	5[b]	12	83	2.502
	E (10.1)		13	87	2.510
	F (10.3)		13	87	2.510
II	Hg−S distance	2.35	2.45	2.52	
	A	95	5		2.355
	B	46	54		2.404
	C	17	60	23	2.449
	D	5[b]	14	81	2.502
	E		16	84	2.509
	F		14	86	2.510
III	Hg−S distance	2.35	2.44	2.53	
	A	94	6		2.355
	B	42	58		2.402
	C	12	62	26	2.453
	D	5[b]	22	73	2.501
	E		24	76	2.508
	F		24	76	2.508
IV	Hg−S distance	2.35	2.45	2.53	
	A	95	5		2.355
	B	46	54		2.404
	C	16	61	23	2.452
	D	5[b]	24	71	2.502
	E		27	73	2.508
	F		26	74	2.509

[a] The average $R = \Sigma$(% of species) × (average Hg−S distance in the species) can be compared to the average distances obtained for solutions A, B, and C and D−F: 2.36, 2.39, 2.44, and 2.50 Å, respectively (Table 3). [b] Estimated from Raman.

XANES of Hg^{II}−Cysteine Solutions. The slightly different X-ray absorption near edge structures (XANES) for solutions A and C (Figure 2a) with increasing H_2Cys/Hg^{II} ratios are consistent with a gradual change in the mercury(II) coordination, while for solutions D and E, with a large excess of the ligand (H_2Cys/Hg^{II} ratios 5.3 and 10.1, respectively), very similar XANES spectra were obtained (Figure 2b). Also, the XANES spectrum of the $[Hg(HCys)_2]$ complex in the solid compound differs somewhat from that of solution A, in which the deprotonated $[Hg(Cys)_2]^{2-}$ complex dominates (see Figure S3).

EXAFS of Hg^{II}−Cysteine Solutions. The k^3-weighted EXAFS oscillations exhibit similar frequency and envelope for solutions A−F, indicating that sulfur is the only significant backscatterer. The Fourier transforms display a single peak representing the Hg−S bonds (Figure 3, right). The peak height decreases and becomes broader from A to C, while for solutions D−F with a high excess of cysteine, the Hg−S peak intensity increases and shifts to a longer distance. EXAFS model curves were simulated for the Hg−S interactions and curve fitted with least-squares methods to

(31) (a) Wasserman, S. R. *J. Phys. IV France* **1997**, *7*, C2−203. (b) Wasserman, S. R.; Allen, P. G.; Shuh, D. K.; Bucher, J. J.; Edelstein, N. M. *J. Synchrotron Rad.* **1999**, *6*, 284.

(32) George, G. N.; George, S. J.; Pickering, I. J. *EXAFSPAK*; Stanford Synchrotron Radiation Laboratory (SSRL): Menlo Park, CA, 2001.

(33) (a) Vosko, S. H.; Wilk, L.; Nusair, M. *Can. J. Phys.* **1980**, *58*, 1200. (b) ADF2004. SCM (http://www.scm.com), Department of Theoretical Chemistry, Vrije Universiteit: Amsterdam, The Netherlands.

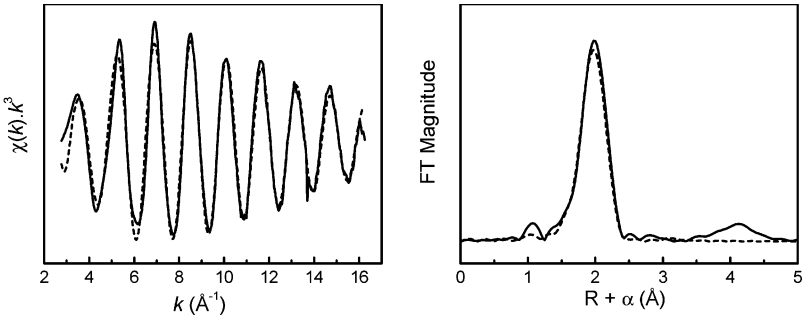

Figure 1. k^3-weighted EXAFS oscillation and corresponding Fourier transform: experimental data (solid line) and model fit (---) for the solid $Hg(HCys)_2$ compound (cf. Table 3). The minor peak at about 4.1 Å (distances not corrected for phase shift) corresponds to multiple scattering in the linear S−Hg−S entity ($n_{leg} = 4$).

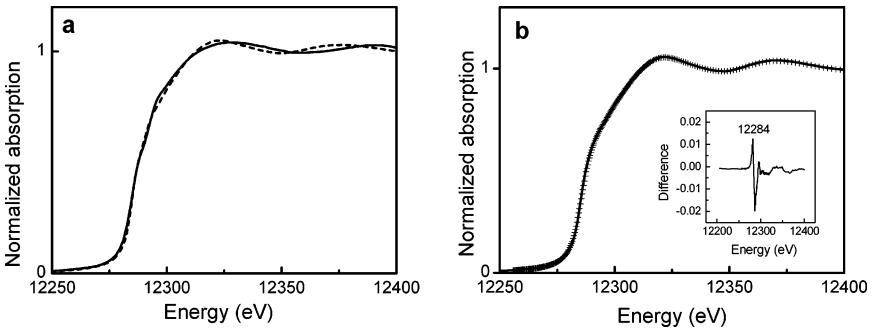

Figure 2. Normalized XANES spectra of Hg^{II}−cysteine solutions: (a) A (—) and C (---) and (b) D (+++) and E (—), with the inset showing their difference (also see Figure S3).

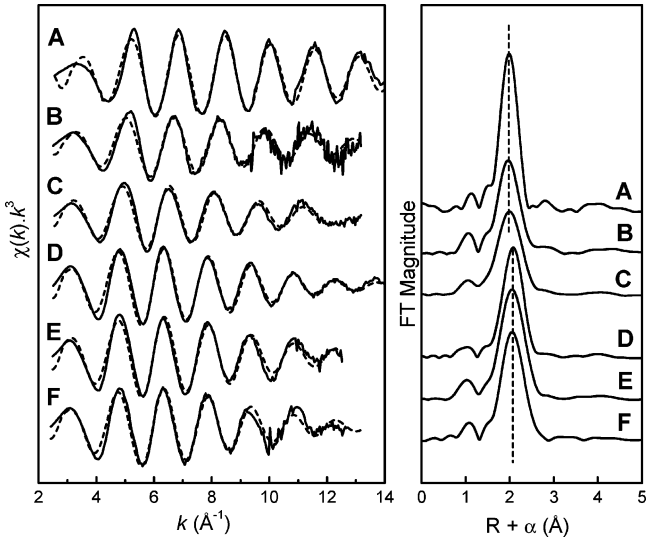

Figure 3. (Left) EXAFS model curves (dashed line) for Hg−S interactions according to Table 3, as compared to the k^3-weighted experimental EXAFS oscillation (solid line) for solutions A−F. (Right) Fourier transforms of the experimental EXAFS spectra without phase shift corrections.

the experimental EXAFS oscillations, which were Fourier-filtered over the Hg−S range to exclude other more distant interactions. The parameters are reported in Table 3, and the resulting model functions are compared with the experimental EXAFS oscillations in Figure 3 (left). The coordination numbers obtained with $S_0^2 = 0.9$ (cf. eq 1) indicate that the two-coordinated $[Hg(Cys)_2]^{2-}$ complex dominates in solution A with the H_2Cys/Hg^{II} ratio of 2.2, with mixtures of higher species formed at higher ratios (Table 3). However, because of the uncertainty in the S_0^2 value, comparisons of the mean metal−ligand bond distance with that obtained for complexes in crystal structures can provide more reliable information on the coordination geometry.[34]

The mean Hg−S bond distance obtained for solution A, 2.36(2) Å, is slightly longer than the value expected from crystal structures for a linear two-coordinated complex (~2.34 Å). The average Hg−S bond distance of 2.44(2) Å for solution C with a H_2Cys/Hg^{II} ratio of 4.3 is within the range expected for a three-coordinated $Hg(SR)_3$ complex (Table 3).[13,14,16,35] It is similar to the Hg−S bond distances found from EXAFS results for the three-coordinated Hg−MerR (2.43(2) Å) and Hg−MT (2.42(2) Å) compounds, [8−11] even though the Raman spectrum of solution **C** displays a small band at 334 cm^{-1} showing that a minor amount of the $[Hg(Cys)_2]^{2-}$ complex remains (see Raman Spectra). For solution B, with the intermediate H_2Cys/Hg^{II} ratio of 3.3, the average Hg−S bond distance obtained, 2.39(2) Å, indicates a mixture of the $[Hg(Cys)_2]^{2-}$ and $[Hg(Cys)_3]^{4-}$ complexes. For solutions D and E with H_2Cys/Hg^{II} ratios from 5.3 to 10.1 (cf. Figure S4), and even for solution F with the highest excess of fully deprotonated Cys^{2-} species (i.e., the H_2Cys/Hg^{II} ratio = 10.3 at pH = 13), the mean Hg−S bond distance of 2.50(2) Å consistently emerges. That Hg−S bond distance is slightly shorter than the average Hg−S bond length (2.52−2.54 Å) observed in the crystal structures of mononuclear $Hg(SR)_4$ species with neutral or 2− charge,[13,14,16] which indicates that a four-coordinated mercury(II) thiolate species is dominating in solutions with $H_2Cys/Hg^{II} > 5$.

(34) Sandström, M.; Persson, I.; Jalilehvand, F.; Lindqvist-Reis, P.; Spångberg, D.; Hermansson, K. *J. Synchrotron Rad.* **2001**, *8*, 657.
(35) Matzapetakis, M.; Farrer, B. T.; Weng, T. C.; Hemmingsen, L.; Penner-Hahn, J. E.; Pecoraro, V. L. *J. Am. Chem. Soc.* **2002**, *124*, 8042.

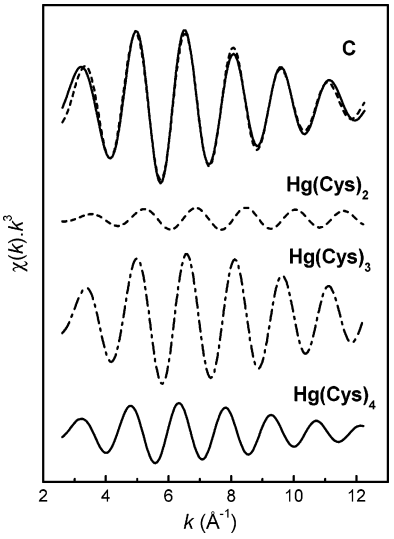

Figure 4. Fourier filtered, k^3-weighted EXAFS oscillation for solution C (top, solid line) fitted to an EXAFS (top, dashed line) model function (III in Table 4) from a linear combination of Hg−S interactions in the $[Hg(Cys)_2]^{2-}$ (12%), $[Hg(Cys)_3]^{4-}$ (62%), and $Hg(Cys)_4$ (26%) species.

For the $[Hg(HCys)_2]$ complex in the solid compound, and for solution A with a dominating $[Hg(Cys)_2]^{2-}$ species, the refinements of EXAFS parameters resulted in ΔE_0 values between 12.2 and 12.5 eV, while the ΔE_0 values varied within the range of 8.6−10.0 eV for solutions B−F. This significant difference is consistent with the less positive mercury atom in the $[Hg(Cys)_3]^{4-}$ and $Hg(Cys)_4$ species.

The low value of the disorder parameter (σ^2) obtained for solution A is close to that for the two-coordinated $[Hg(HCys)_2]$ complex in the solid compound and should mainly reflect the thermally induced variation in the bond length (Table 3). For solutions with higher H_2Cys/Hg^{II} ratios, the Hg−S bond length increases. The σ^2 values increase substantially for solutions B−F, which not only contain three- and four-coordinated Hg^{II}−cysteine species, but also the distribution of distances in mixtures of species will contribute to the high σ^2 values.

To evaluate the relative amount of the Hg^{II}−cysteine species in solutions A−F, EXAFS model spectra were simulated (see Experimental Procedures) using the FEFF 8.1 program, for the three standard species $[Hg(Cys)_2]^{2-}$, $[Hg(Cys)_3]^{4-}$, and $Hg(Cys)_4$, for a range of possible Hg−S bond distances, Debye−Waller parameters (σ^2), and ΔE_0 values (cf. Table 2). Satisfactory fits were obtained by fitting linear combinations of these simulated EXAFS spectra to the experimental EXAFS oscillations by keeping the Hg−S bond distances at 2.35, 2.44−2.45, and 2.52−2.53 Å and the corresponding Debye−Waller parameters at $\sigma^2 = 0.003$, 0.006, and 0.008 Å^2, for the $[Hg(Cys)_2]^{2-}$, $[Hg(Cys)_3]^{4-}$, and $Hg(Cys)_4$ models, respectively (Table 4 and Figures 4 and S5). For the two-coordinated $[Hg(Cys)_2]^{2-}$ complex, the Hg−S bond distance is similar to the average bond length of the $[Hg(HCys)(H_2Cys)]Cl\cdot 0.5H_2O$ crystal structure, 2.34 Å,[15] and that of $[Hg(CH_3)(HCys)]\cdot H_2O$, 2.352 Å,[30] and also for $Hg(SEt)_2$, 2.35(3) Å, from an EXAFS study.[36] For the $[Hg(Cys)_3]^{4-}$ species, the Hg−S bond distance is in good agreement with the mean Hg−S distance of 2.44 Å in the $Hg(SR)_3$ species.[13,14,16,35]

For $Hg(Cys)_4$, the Hg−S bond distance is within the range of 2.52−2.54 Å as expected for $Hg(SR)_4$ species and close to the Hg−S distance, 2.514(2) Å, recently reported for the four-coordinated $Hg(DMPS)_4$ complex (DMPS = dimercaptopropanesulfonic acid) in an EXAFS study.[37] Also, when the Hg−S distance of 2.51 Å was tested for the $Hg(Cys)_4$ species in solutions D−F, a satisfactory fit could be obtained; however, the percentage then rose to above 95%, which does not seem realistic based on the ^{199}Hg NMR data. These analyses show that the two-coordinated $[Hg(Cys)_2]^{2-}$ complex is the major species in solution A, while solutions D−F with a substantial excess of free Cys^{2-} show similar compositions with $Hg(Cys)_4$ dominating, as expected from their similar Hg−S bond distances and XANES spectra (Tables 3 and 4 and Figure 2b).

The small amount remaining of the linear $[Hg(Cys)_2]^{2-}$ complex in solution D has been estimated from Raman measurements. The ^{199}Hg NMR spectra show that the amount of $Hg(Cys)_4$ in solution E with the H_2Cys/Hg^{II} ratio of 10.3 is somewhat higher than in solution D with a H_2Cys/Hg^{II} ratio of 5.3. These spectroscopic analyses are valuable complements to the EXAFS approach, which is not sensitive enough to detect small variations (about ±10%) in the amount of the four-coordinated species.

^{199}Hg NMR Spectra. The isotropic shift of mercury(II) thiolates in solution generally decreases as the coordination number increases. With $Hg(CH_3)_2$ as reference, $\delta(^{199}Hg) = 0$, the chemical shift for two-coordinated mercury(II) thiolates normally fall in the range of −1200 to −800 ppm, depending on the solvent.[13] For a series of $[Hg(SR)_4]^{2-}$ complexes, the reported $\delta(^{199}Hg)$ values in 1:1 H_2O/D_2O solutions lie in the range of −585 to −270 ppm.[13,38] For two structurally characterized three-coordinated mercury thiolates, $[Hg(S\text{-}t\text{-}Bu)_3]^-$ and $[Hg(SPh)_3]^-$, ^{199}Hg chemical shifts were reported at −157 and −354 ppm in dimethyl sulfoxide solution, respectively;[39] thus partly within the range of four-coordinated species.

Figure 5 shows the ^{199}Hg NMR spectra of solutions A−D and G−I, with chemical shifts of −609 (A), −464 (B), −426 (C), −378 (D), −362 (G), −357 (H), and −350 ppm (I). Because of the high lability of mercury(II) thiolates, the ligand exchange is rapid on the NMR time scale, and an average isotropic shift is observed for all Hg(II) species present in the solution. While the total Hg(II) concentration (∼0.09 mol dm^{-3}) is similar in all 1:10 D_2O/H_2O solutions, the shielding decreases with a less negative isotropic shift as the H_2Cys/Hg^{II} ratio increases. This deshielding is more drastic from solution A (ratio 2.3) to D (ratio 5.3) and from solution D−I (ratio 11.5) asymptotically approaches a value of ∼ −340 ppm, which should correspond to the chemical

(36) Raybuck, S. A.; Distefano, M. D.; Teo, B. K.; Orme-Johnson, W.; Walsh, C. T. *J. Am. Chem. Soc.* **1990**, *112*, 1983.
(37) George, G. N.; Prince, R. C.; Gailer, J.; Buttigieg, G. A.; Denton, M. B.; Harris, H. H.; Pickering, I. J. *Chem. Res. Toxicol.* **2004**, *17*, 999.
(38) Carson, K. G.; Dean, P. A. W. *Inorg. Chim. Acta* **1982**, *66*, 157.
(39) Natan, M. J.; Millikan, C. F.; Wright, J. G.; O'Halloran, T. V. *J. Am. Chem. Soc.* **1990**, *112*, 3255.

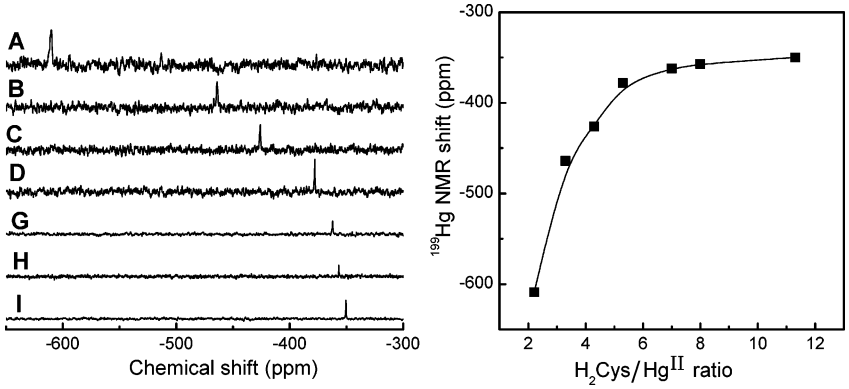

Figure 5. (Left) ^{199}Hg NMR spectra of solutions A−D and G−I. (Right) Variation of the ^{199}Hg NMR chemical shift vs the H_2Cys/Hg^{II} ratio.

shift of the $Hg(Cys)_4$ species. This implies that the $[Hg(Cys)_2]^{2-}$ species gradually is converted to three- and four-coordinated species when increasing the H_2Cys/Hg^{II} ratio. The ^{199}Hg chemical shift of the $[Hg(Cys)_3]^{4-}$ complex is likely to be about 80−90 ppm lower than that for the $Hg(Cys)_4$ species, also judging from the amounts present in solutions C and D (Table 4). Thus, the ^{199}Hg NMR results support that an amount of 10−15% of the $[Hg(Cys)_3]^{4-}$ complex remains in solution I.

Raman Spectra. An intense polarized Raman band in the range of 245−394 cm^{-1} corresponds to the S−Hg−S symmetric stretching in linearly coordinated Hg^{II}−thiol species,[13] with the shift in the vibrational frequency primarily depending on the effective mass of the ligand. For the solid compound $[Hg(HCys)(H_2Cys)]Cl\cdot 0.5H_2O$, this S−Hg−S mode was found at 316 cm^{-1} [40] (i.e., at the same wavenumber as for the $Hg(HCys)_2$ compound in the present work (cf. Figure S6)). For mercury(II) complexes of cysteine-containing oligopeptides in the solid state, an S−Hg−S stretching band has been reported at 326 cm^{-1}.[41]

Hence, the distinct Raman band at 334 cm^{-1} for solution A with a H_2Cys/Hg^{II} ratio of 2.2 could safely be assigned as the symmetric S−Hg−S stretching vibrational mode of the $[Hg(Cys)_2]^{2-}$ complex (cf. Figures 6 and S6). The EXAFS results show that in solution A about 95% of the total Hg^{II} concentration is in the form of $[Hg(Cys)_2]^{2-}$ complexes (Table 4). The curve-fitted peak area of the Raman band at 334 cm^{-1} (cf. Figure S7) then allows the relative amount of the $[Hg(Cys)_2]^{2-}$ complexes to be estimated, with the Cl−O symmetric stretching band at 933 cm^{-1} of the perchlorate ion used for internal intensity calibration. The results, 39% in solution B, 12% in C, and 5% in D, are in reasonable agreement with the EXAFS values (Table 5). For solutions E and F with a higher excess of cysteine, the 334 cm^{-1} Raman band is below noise level, indicating less than 5% $[Hg(Cys)_2]^{2-}$.

With increasing H_2Cys/Hg^{II} ratio for solutions A−F, a minor broad band appears at about 277 cm^{-1}, which shifts to lower frequencies, and increases in intensity. Curve fitting could resolve this band into two components at about 285 and 265 cm^{-1}, which tentatively can be assigned to the symmetric Hg−S stretching modes of the $Hg(Cys)_3^{4-}$ and $Hg(Cys)_4$ species, respectively (cf. Figure S7). For trigonal $Hg-S_3$ coordination in the $[Hg(SMe)_3]^-$ complex and the Hg^{II}−MerR regulatory protein, a Raman band at 282 cm^{-1} has been ascribed to an essentially pure Hg−S stretching vibrational mode, while for the $[Hg(S\text{-}t\text{-}Bu)_3]^-$ complex, a much lower frequency, 207 cm^{-1}, is obtained.[42]

The C−S stretching in the pure cysteine solution at pH = 11 (Cys^{2-}) occurs at 686 cm^{-1} and shifts only slightly to 684 cm^{-1} in solutions C and D with excess of Cys^{2-}. For solutions A and B, the shift to lower frequencies, 682 and 678 cm^{-1}, respectively, becomes apparent with decreasing intensity when the Hg^{II}−S bonding weakens the C−S bond in the coordinated cysteine ligands (cf. Figure 6). The corresponding vibrational mode has been reported at 678, 682, and 670 cm^{-1} for the solid compounds L-cysteine, $H_2Cys\cdot HCl\cdot H_2O$, and $[Hg(HCys)(H_2Cys)]Cl\cdot 0.5H_2O$, respectively.[40] The Raman bands at 630 and 462 cm^{-1} are the deformation modes of ClO_4^-.[26]

Table 5. Probable Distribution of the Relative Amount of $[Hg(Cys)_n]$ Species, n = 2, 3, 4 (see Figure S5), Based on the Combined Results from EXAFS, ^{199}Hg NMR, and Raman[a]

solution (ratio)	$[Hg(Cys)_2]^{2-}$ from Raman (%)	$[Hg(Cys)_2]^{2-}$ (%)	$[Hg(Cys)_3]^{4-}$ (%)	$Hg(Cys)_4$ (%)
A (2.2)	94[b]	94	6	
B (3.3)	39	42	58	
C (4.3)	12	12	62	26
D (5.3)	5	5[c]	22	73
E (10.1)	<1		∼15	∼85

[a] Estimated error: ±10% in the reported values according to EXAFS fitting model III in Table 4. The $[Hg(Cys)_2]^{2-}$ amount is obtained from the Raman S−Hg−S symmetric stretching band at 334 cm^{-1}. [b] Fixed at the EXAFS value. [c] Estimated from Raman.

Electronic Spectra. In the UV−vis absorption spectra of the solutions A−D and J, the $\Delta\epsilon$ value ($= \epsilon_{Hg-Cys} - \epsilon_{Cys}$) represents the absorption of mercury(II) species (cf. Figure S8). Solution J with a H_2Cys/Hg^{II} ratio of 2.0 is dominated by a linear $[Hg(Cys)_2]^{2-}$ species, and K contains pure cysteine (2 mmol dm^{-3}) at pH = 10.4.[43] For the solutions A−D, the increasing amount of $[Hg(Cys)_3]^{4-}$ and $Hg(Cys)_4$ species shifts the absorption toward higher wavelengths

(40) Sze, Y. K.; Davis, A. R.; Neville, G. A. *Inorg. Chem.* **1975**, *14*, 1969.
(41) Ueyama, N.; Nakata, M.; Nakamura, A. *Bull. Chem. Soc. Jpn.* **1985**, *58*, 464.
(42) Fleissner, G.; Kozlowski, P. M.; Vargek, M.; Bryson, J. W.; O'Halloran, T. V.; Spiro, T. G. *Inorg. Chem.* **1999**, *38*, 3523.
(43) Nishino, H.; Kosaka, A.; Hembury, G. A.; Matsushima, K.; Inoue, Y. *J. Chem. Soc., Perkin Trans. 2* **2002**, 582.

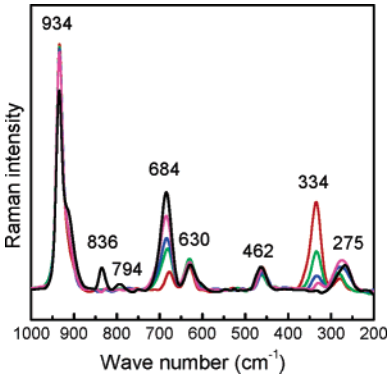

Figure 6. Raman spectra of solutions A (red), B (green), C (blue), D (pink), and E (black), after background subtraction and internal intensity calibration by means of the perchlorate Cl−O symmetric stretching (934 cm^{-1}) band (for concentrations, see Table 1).

(Table 4). However, the absorption of solution D, where the $Hg(Cys)_4$ species dominates, is very similar to that of solution C with about 60% $[Hg(Cys)_3]^{4-}$ and does not allow the $[Hg(Cys)_3]^{4-}$ and $Hg(Cys)_4$ species to be distinguished.

Conclusions

The EXAFS analyses show three sulfur-bonded mononuclear $Hg(Cys)_n$ ($n = 2, 3, 4$) species in alkaline aqueous solutions with Hg^{II} ~0.09 mol dm^{-3} and H_2Cys/Hg^{II} ratios from 2 to 11.5. The novel four-coordinated complex, $Hg(Cys)_4$, with the mean Hg−S bond distance obtained as 2.52(2) Å, is the dominating species in solutions with high H_2Cys/Hg^{II} ratios (>5). The mean Hg−S bond distances of the previously reported $[Hg(Cys)_2]^{2-}$ and $[Hg(Cys)_3]^{4-}$ complexes have been determined to be 2.35(2) and 2.44(2) Å, respectively, by deconvoluting the EXAFS oscillations. UV−vis, Raman, and ^{199}Hg NMR spectroscopic characterizations support the EXAFS results. The strongly coordinated linear $[Hg(Cys)_2]^{2-}$ complex has a distinct S−Hg−S symmetric stretching Raman band at 334 cm^{-1}, which has been used to derive the minor amount that still can be discerned in solutions with an excess of cysteine. For solutions with H_2Cys/Hg^{II} ratios of 4.3 and 5.3, the remaining $[Hg(Cys)_2]^{2-}$ amount was found to be 10 and 5 mmol dm^{-3}, respectively. ^{199}Hg NMR provides a more sensitive tool for tracking small variations in the amount of $[Hg(Cys)_3]^{4-}$ and $Hg(Cys)_4$ species than the average Hg−S bond distance resulting from the EXAFS investigations. Table 5 provides the proposed distribution of $[Hg(Cys)_n]$ ($n = 2, 3$, and 4) species in alkaline aqueous solution. A fair account of the distribution found for the $[Hg(Cys)_2]^{2-}$, $[Hg(Cys)_3]^{4-}$, and $Hg(Cys)_4$ species in Table 5 is obtained by assuming the stability constants $\log \beta_n = 40.0$, 41.3, and 42.4, respectively, for the formation of the Hg^{II}−cysteine complexes according to the equilibria: $Hg^{2+} + nCys^{2-} \rightleftarrows Hg(Cys)_n$ with $n = 2$, 3, and 4 (cf. Figure S9); thus, the successive stability constants K_3 and K_4 are about 20 and 13 M^{-1}, respectively, for the weak complex formation of the $[Hg(Cys)_3]^{4-}$ and $Hg(Cys)_4$ species. Because only mononuclear species are formed, the results are representative also for systems with low mercury concentrations. The activity of free cysteine (or equivalent activity of thiol groups) will be the main factor determining the Hg^{II}−cysteine species present in solution.

Acknowledgment. We thank Prof. Derek Peak, University of Saskatchewan, for use of the FT-Raman instrument. X-ray absorption measurements were carried out at the Photon Factory, Tsukuba, Japan (Proposal 2003G286), and Stanford Synchrotron Radiation Laboratory (SSRL), a U.S. national user facility operated by Stanford University on behalf of the U.S. Department of Energy, Office of Basic Energy Sciences (Proposal 2848). We gratefully acknowledge the Natural Sciences and Engineering Research Council (NSERC) of Canada, Canada Foundation for Innovation (CFI), and the Province of Alberta (Department of Innovation and Science) for providing financial support. F.J. is a recipient of the NSERC University Faculty Award (UFA).

Supporting Information Available: Table of eigenvalues obtained from EXAFS PCA analysis, figures showing structures for $Hg(Cys)_n$ ($n = 2, 3, 4$) optimized by means of the Amsterdam Density Functional (ADF) program, XANES and Raman spectra of solid $Hg(HCys)_2$ and solutions A−E, curve-fitting of EXAFS and Raman spectra of solutions A−D, UV−vis spectra of solutions A−D, J, and K, and the fraction diagram of $Hg(Cys)_n$ species ($n = 1-4$). This material is available free of charge via the Internet at http://pubs.acs.org.

IC0508932